3. Thermal Bremsstrahlung

3.1 Classical Treatment with Quantum Corrections

References to original papers:

- Oster, L., *Rev. Mod. Phys.*, **33**, 525, 1961
- Scheuer, P. A. G., *M.N.R.A.S.*, **120**, 231, 1960

Free-free radiation occurs when electrons are deflected in their motion by ions of *positive* charge. (Note that particles of like charge produce no dipole radiation.) In the classical treatment, we assume (at least initially) that $h\nu \ll kT$ which corresponds to the "weak" scattering limit wherein impact parameters are large and deflection angles small. For very small impact parameters, on the other hand, quantum effects become important, making two-body hyperbolic orbits and classical radiation theory no longer valid. It turns out that not only the high-frequency portion of the bremsstrahlung spectrum involves small impact parameters but the high-temperature limit as well. High T is associated with high particle velocities which can lead to radiation at a given frequency only for small impact parameters.

We follow (more or less) Oster's treatment which differs somewhat from the text (Rybicki & Lightman).

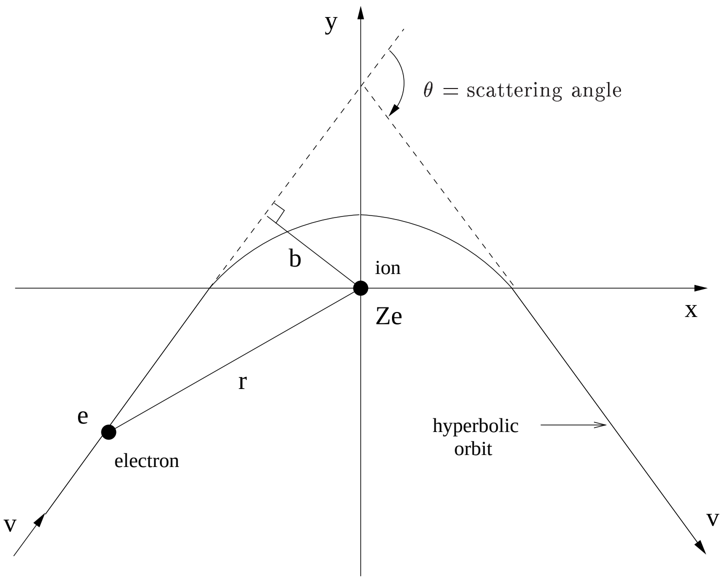

Figure 3.11 – The hyperbolic trajectory of an electron scattered by the Coulomb force of an ion. The impact parameter is b, the initial and final speed of the electron relative to the ion is v, and by design $x = 0$ at $t = 0$. The scattering angle θ can easily be calculated from 2-body dynamics.

The spectrum, $dW/d\nu$, of the emitted radiation from *one* electron is given in terms of the Fourier transforms of the accelerations $\ddot{x}(t)$ and $\ddot{y}(t)$:

$$\frac{dW}{d\nu} = \frac{4e^2}{3c^3} \left[|\widehat{\ddot{x}}(\nu)|^2 + |\widehat{\ddot{y}}(\nu)|^2 \right] .$$

The acceleration transforms are sharp pulses due to the brief nature of the electron-ion encounter.

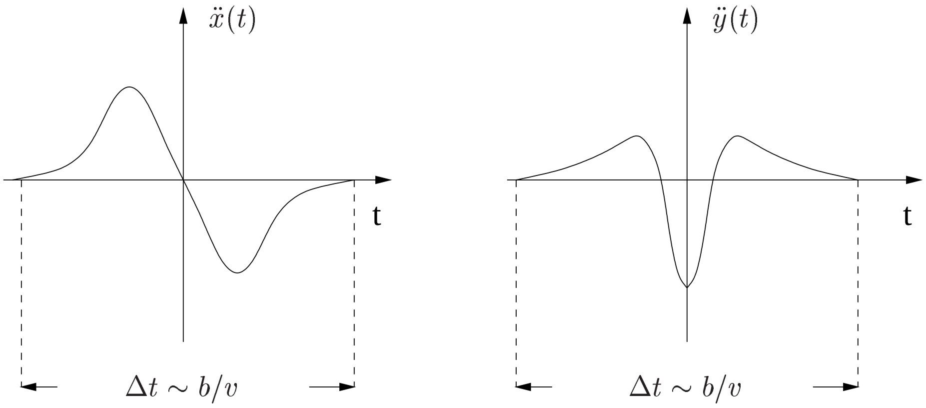

Setting $\Delta t = b/v$, we note that $\ddot{x}(t)$ and $\ddot{y}(t)$ tend to zero when $|t|$ exceeds Δt, and also that $\widehat{\ddot{x}}(\nu)$ and $\widehat{\ddot{y}}(\nu)$ are nonzero only when $2\pi\nu\,\Delta t \leq 1$; that is, $\widehat{\ddot{x}}(\nu) \to 0$ when $2\pi\nu\,\Delta t > 1$.

Consider the low frequency regime: $2\pi\nu\,\Delta t \ll 1$. Then,

$$\begin{aligned} \widehat{\ddot{x}}(\nu) &= \int_{-\infty}^{\infty} \ddot{x}(t)\,dt &= \Delta\dot{x}\ , \\ \widehat{\ddot{y}}(\nu) &= \int_{-\infty}^{\infty} \ddot{y}(t)\,dt &= \Delta\dot{y}\ . \end{aligned}$$

Thus,

$$|\widehat{\ddot{x}}(\nu)|^2 + |\widehat{\ddot{y}}(\nu)|^2 = \Delta\dot{x}^2 + \Delta\dot{y}^2 = |\boldsymbol{\Delta v}|^2$$

where $\boldsymbol{\Delta v}$ is the change in the velocity:

$$\begin{aligned} |\boldsymbol{\Delta v}|^2 = |\boldsymbol{v}_{\text{final}} - \boldsymbol{v}_{\text{init}}|^2 &= \boldsymbol{v}_f \cdot \boldsymbol{v}_f + \boldsymbol{v}_i \cdot \boldsymbol{v}_i - 2\boldsymbol{v}_f \cdot \boldsymbol{v}_i \\ &= 2v^2 - 2v^2\cos\theta \\ &= 2v^2\,(1 - \cos\theta)\ . \end{aligned}$$

Now use $1 - \cos\theta \equiv 2\sin^2\frac{\theta}{2}$ to get

$$\frac{dW}{d\nu} = \frac{16e^2}{3c^3}\,v^2\,\sin^2\frac{\theta}{2}\ .$$

Next invoke the "Rutherford Scattering" formula:

$$\tan\frac{\theta}{2} = \frac{Ze^2}{mv^2 b}$$

together with

$$\frac{\sin^2\frac{\theta}{2}}{1 - \sin^2\frac{\theta}{2}} = \tan^2\frac{\theta}{2} = \left(\frac{Ze^2}{mv^2 b}\right)^2$$

to yield

$$\sin^2\frac{\theta}{2} = \left[1 + \left(\frac{mv^2 b}{Ze^2}\right)^2\right]^{-1}$$

and

$$\frac{dW}{d\nu} = \frac{16e^2v^2}{3c^3}\left[1+\left(\frac{mv^2b}{Ze^2}\right)^2\right]^{-1} \qquad \left(\nu \ll \frac{v}{2\pi b}\right).$$

We can now make a plot of the energy per unit bandwidth for a single encounter:

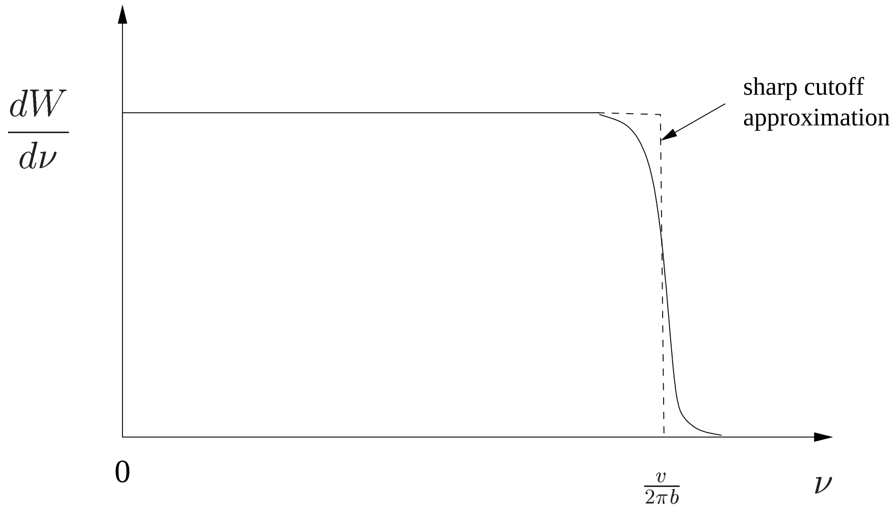

Next, assume that we have a bunch of electrons with a velocity distribution given by $f(v)$, say. What is the total energy radiated per unit bandwidth, per unit time, per unit solid angle, per unit volume in a plasma with ion density n_i and electron density n_e? To answer this question, consider all the electrons with velocity v. The number of encounters per unit time with impact parameter between b and $b+db$ and velocity between v and $v+dv$ is

$$n_i n_e v \times 2\pi b\, db \times f(v)\, dv \qquad \text{(per unit volume)}$$

and so

$$\begin{aligned}\frac{dW}{d\nu\, dv\, dt\, dV\, d\Omega} &= \frac{n_i n_e f(v) v}{4\pi}\int_{b_{\min}}^{b_{\max}} \frac{dW}{d\nu}\, 2\pi b\, db \\ &= \frac{4Z^2e^6 n_i n_e f(v)}{3m^2c^3v}\ln\left[1+\left(\frac{mv^2b}{Ze^2}\right)^2\right]_{b_{\min}}^{b_{\max}}.\end{aligned}$$

The log term is normally absorbed into the free-free Gaunt factor, $g_{\rm ff}$; thus,

$$\frac{dW}{d\nu\, dv\, dt\, dV\, d\Omega} = \frac{8\pi Z^2e^6 n_i n_e f(v)}{3\sqrt{3}m^2c^3v}\, g_{\rm ff}(\nu, v)$$

where

$$g_{\rm ff}(\nu, v) \equiv \frac{\sqrt{3}}{2\pi}\ln\left[1+\left(\frac{mv^2b}{Ze^2}\right)^2\right]_{b_{\min}}^{b_{\max}}.$$

Clearly, there is no problem in setting $b_{\min}=0$. However, we can't replace $b_{\max}$ by ∞. The blow-up at the high limit is due to the assumption that even very distant encounters are all independent of one another. In actual fact, distant encounters are simultaneous and not sequential – their effects tend to cancel one another and are certainly not additive. But there is a realistic upper limit that can be imposed. Recall that $dW/d\nu$ is nonzero only when

$$\nu < \frac{v}{2\pi b} \qquad \Longrightarrow \qquad b < \frac{v}{2\pi\nu} \qquad \Longrightarrow \qquad b_{\rm max} = \frac{v}{2\pi\nu} \ .$$

Thus, the Gaunt factor becomes

$$g_{\rm ff}(\nu, v) \equiv \frac{\sqrt{3}}{2\pi} \ln \left[1 + \left(\frac{mv^3}{2\pi Z e^2 \nu} \right)^2 \right] \ .$$

To obtain the thermal emission coefficient, we integrate over a Maxwellian velocity distribution:

$$j_\nu = \int_{v_{\rm min}}^{\infty} \left(\frac{dW}{d\nu\, dv\, dt\, dV\, d\Omega} \right) dv$$

with

$$f(v)\, dv = \left(\frac{2}{\pi} \right)^{1/2} \left(\frac{m}{kT} \right)^{3/2} v^2\, {\rm e}^{-mv^2/2kT}\, dv \ .$$

There is a velocity minimum here (given by $mv_{\rm min}^2 = 2h\nu$) because electrons with lower kinetic energy cannot emit photons of energy $h\nu$. Carrying out the integral, one finds an exponential cutoff in j_ν which is due, of course, to the same cutoff in $f(v)$:

$$j_\nu = \frac{8}{3} \left(\frac{2\pi}{3} \right)^{1/2} \frac{Z^2 e^6}{m^2 c^3} \left(\frac{m}{kT} \right)^{1/2} n_i n_e\, {\rm e}^{-h\nu/kT}\, \bar{g}_{\rm ff}(\nu, T)$$

where

$$\bar{g}_{\rm ff}(\nu, T) = \frac{\sqrt{3}}{\pi} \ln \left[\left(\frac{2}{\gamma} \right)^{3/2} \left(\frac{kT}{m} \right)^{1/2} \left(\frac{kT}{2\pi Z e^2 \nu} \right) \right]$$

and

$$\gamma \equiv \text{Euler's constant} = 1.781 \ .$$

Note that the exponent $\frac{3}{2}$ in $\bar{g}_{\rm ff}$ would be $\frac{5}{2}$ if we didn't use the sharp cutoff approximation for $b_{\rm max}$. Also, note that the integration above has been facilitated by assuming that quantity inside the log term in $\bar{g}_{\rm ff}$ is much larger than unity, so only the second term in the square bracket is retained.

The formula for j_ν has a number of restrictions attached to it which, in effect, makes it a "classical" formula:

(i) It was assumed that $h\nu \ll kT$.

(ii) Also, in the same integration, it was assumed that

$$\frac{mv^2 b_{\rm max}}{Ze^2} = \frac{mv^3}{2\pi Z e^2 \nu} \gg 1 \ .$$

Looking back at the Rutherford scattering formula, this is equivalent to assuming only *small angle scatterings*. The assumption allows us to ignore the '1' in the argument of the log for $g_{\rm ff}(\nu, v)$. Replace v in the above inequality by $v_{\rm rms} = (2kT/m)^{1/2}$. Then,

$$\frac{h\nu}{kT} \ll \left(\frac{kT}{Z^2 R_y} \right)^{1/2}$$

where the Rydberg constant $R_y \equiv 2\pi^2 me^4/h^2 = 13.6\,{\rm ev}$ has units of energy.

(iii) It turns out that there *is* a problem with setting $b_{\text{min}} = 0$. This is because the classical treatment is not valid when $b_{\text{min}} < h/mv$ which is the deBroglie wavelength of the electron. In particular, the orbit past the ion is no longer classical. However, we can safely use $b_{\text{min}} = 0$ if

$$\frac{mv^2 b_{\text{min}}}{Ze^2} \ll 1 \quad \text{with} \quad b_{\text{min}} = \frac{h}{mv}$$

which is equivalent to

$$v \ll \frac{Ze^2}{h} \qquad (\text{limit on } v \text{ or } T)\ .$$

Applying this limit to v_{rms}, we have

$$\frac{kT}{Z^2 R_y} \ll \frac{1}{4\pi^2} < 1 \quad \Longrightarrow \quad \frac{h\nu}{kT} \ll \left(\frac{kT}{Z^2 R_y}\right)^{1/2} \ll 1\ .$$

Note that restrictions (ii) and (iii) imply (i).

What we have derived here is an expression for the Gaunt factor which is good only in the low ν, low T portion of the (ν, T)-plane; i.e., the lower left-hand corner of Fig. 5.2 on p160 of the text. However, one can consider our expression for j_ν, the thermal free-free emission coefficient, good for all regimes if the necessary correction factors (quantum-mechanical and otherwise) are all incorporated into $\bar{g}_{\text{ff}}$. Such a general Gaunt factor falls in the range 0.25-5.5 (see figure below) but in most practical situations it is within a factor 2 of unity.

Figure 3.12 – Numerical values of the Gaunt factor $\bar{g}_{\text{ff}}(\nu, T)$. Here the frequency variable is $u = 4.8 \times 10^{-11}\nu/T$ and the temperature variable is $\gamma^2 = 1.58 \times 10^5 Z^2/T$. The classical regime corresponds to $u < 1$ and $\gamma^2 > 40$. (Taken from W. Karzas & R. Latter 1961, *Ap.J. Suppl.*, **6**, 167.)

Useful Formulae at Radio Frequencies

Substituting numerical values for the basic constants, we find that the emission coefficient becomes

$$j_\nu = 5.44 \times 10^{-39} \frac{Z^2 n_i n_e}{T^{1/2}} \, \mathrm{e}^{-h\nu/kT} \, \bar{g}_{\mathrm{ff}}(\nu, T) \qquad \mathrm{ergs\,s^{-1}\,cm^{-3}\,Hz^{-1}\,sr^{-1}}$$

where

$$\bar{g}_{\mathrm{ff}}(\nu, T) = \frac{\sqrt{3}}{\pi} \left[17.7 + \ln\left(\frac{T^{3/2}}{Z\nu}\right) \right] \qquad (h\nu \ll kT \ll Z^2 R_y / 4\pi^2) \ .$$

The corresponding emissivity is given by

$$\begin{aligned} \epsilon_{\mathrm{ff}} &= 4\pi \int_0^\infty j_\nu \, d\nu \\ &= \frac{32\pi e^6}{3kmc^3} \left(\frac{2\pi kT}{3m}\right)^{1/2} Z^2 n_e n_i \, \bar{g}_{\mathrm{B}}(T) \\ &= 1.4 \times 10^{-27} \, T^{1/2} n_e n_i Z^2 \, \bar{g}_{\mathrm{B}}(T) \qquad \mathrm{ergs\,s^{-1}\,cm^{-3}} \end{aligned}$$

where $\bar{g}_{\mathrm{B}}$ is a mean of $\bar{g}_{\mathrm{ff}}$ over frequency; it generally falls in the range 1.1-1.5.

The free-free absorption coefficient $\alpha_\nu(\mathrm{ff})$ may be found from Kirchoff's Law:

$$\begin{aligned} \alpha_\nu = \frac{j_\nu}{B_\nu} &= j_\nu \left(\frac{c^2}{2h\nu^3}\right) \left(\mathrm{e}^{h\nu/kT} - 1\right) \\ &= 3.69 \times 10^8 \, \frac{Z^2 n_i n_e}{T^{1/2} \nu^3} \, (1 - \mathrm{e}^{-h\nu/kT}) \, \bar{g}_{\mathrm{ff}}(\nu, T) \quad \mathrm{cm^{-1}} \\ &\rightarrow 1.81 \times 10^{-2} \, \frac{Z^2 n_i n_e}{T^{3/2} \nu^2} \, \bar{g}_{\mathrm{ff}}(\nu, T) \quad \mathrm{cm^{-1}} \quad (\mathrm{h}\nu \ll \mathrm{kT} \ll \mathrm{Z^2 R_y}/4\pi^2) \ . \end{aligned}$$

Note the ν^{-2} dependence for the absorption coefficient at radio frequencies. This is the *net* value, corrected for stimulated emission.

A very useful expression for the optical depth $\tau_\nu = \int \alpha_\nu \, ds$ may be obtained from a power-law fit to the (ν, T)-dependence of the Gaunt factor (see Rohlfs, K., *Tools of Radio Astronomy*, p178-179).

$$\tau_\nu = 8.235 \times 10^{-2} \, T^{-1.35} \nu^{-2.1} \, E_{\mathrm{M}} \, a(\nu, T) \quad (T \text{ in } ^\circ\mathrm{K}, \ \nu \text{ in GHz})$$

where E_{M} is the "emission measure" in $\mathrm{pc\,cm^{-6}}$; it is given by

$$E_{\mathrm{M}} \equiv Z^2 \int_0^s n_i n_e \, ds' \quad \text{(single ionic species)} \ .$$

In the formula for τ_ν, $a(\nu, T)$ is of order unity (see Rohlfs).

These formulae could be adapted to any frequency regime by replacing the analytical expression for $\bar{g}_{\mathrm{ff}}$ by the exact numerical relationship from the Karzas & Latter paper.

3.2 CASE STUDY: HII Regions at Radio Wavelengths

References:

- Rohlfs, K., *Tools of Radio Astronomy*
- Scheffler, H. & Elsässer, H., *Physics of the Galaxy and Interstellar Matter*
- Verschuur, G. L. & Kellerman, K. I. (eds), *Galactic and Extragalactic Astronomy* (Ch. 2)

Provided the background radiation is weak and the source function (or temperature) is a constant, the solution of the transfer equation for thermal radiation looks like

$$I_\nu = B_\nu(T_e)\,(1 - \mathrm{e}^{-\tau_\nu}) \qquad \text{or} \qquad T_b = T_e\,(1 - \mathrm{e}^{-\tau_\nu}) \ .$$

Note that the brightness temperature T_b depends on *both* the kinetic temperature T_e (typically $10^4\,^\circ$K) and the optical depth of the HII region.

Low ν:

At sufficiently low frequency, $\tau_\nu \gg 1$ and, therefore, $T_b \to T_e$ and

$$F_\nu = \int_{\Omega_s} I_\nu\, d\Omega \simeq B_\nu \Omega_s$$

where Ω_s is the solid angle subtended by the source. In the radio regime, $B_\nu \propto \nu^2 T \implies F_\nu \propto \nu^2 T$. Thus, the flux increases with the temperature in the optically thick limit.

High ν:

At high frequency, on the other hand, $\tau_\nu \ll 1$ and, therefore, $T_b \to T_e \tau_\nu$ and

$$F_\nu = \int_{\Omega_s} I_\nu\, d\Omega \simeq B_\nu \int_{\Omega_s} \tau_\nu\, d\Omega \ .$$

But

$$\begin{aligned} \int_{\Omega_s} \tau_\nu\, d\Omega &\propto T_e^{-1.35} \nu^{-2.1} Z^2 \int_{\Omega_s} \int_0^s n_i n_e \left(\frac{dA}{D^2}\right) ds' \\ &\propto T_e^{-1.35} \nu^{-2.1} Z^2 D^{-2} \int_V n_i n_e\, dV \ . \end{aligned}$$

Substituting, we obtain

$$F_\nu = 2.01 \times 10^4\, T^{-0.35} \nu^{-0.1} Z^2 D^{-2} \int_V n_i n_e\, dV \ \propto \ D$$

where F_ν is in units of $\mathrm{J_y}$ ($1\,\mathrm{J_y} \equiv 10^{-26}\,\mathrm{watts\,m^{-2}\,Hz^{-1}} = 10^{-23}\,\mathrm{ergs\,s^{-1}\,cm^{-2}\,Hz^{-1}}$), ν is in Hz, D is in pc, and the density integral is in the unorthodox units of $\mathrm{cm^{-6}\,pc^3}$. The strange temperature dependence of the flux is due to the product of B_ν ($\propto T$) and τ_ν ($\propto T^{-1.35}$).

Strictly speaking, we should sum over all ionic species contributing to the thermal bremsstrahlung but keep in mind that the main contributors are ionized hydrogen and singly ionized helium. That is, we should replace $Z^2 \int n_i n_e\, dV$ by

$$\sum_{j=1}^{N} Z_j^2 \int_V n_{ij} n_e\, dV \ .$$

Spectrum of an H II Region

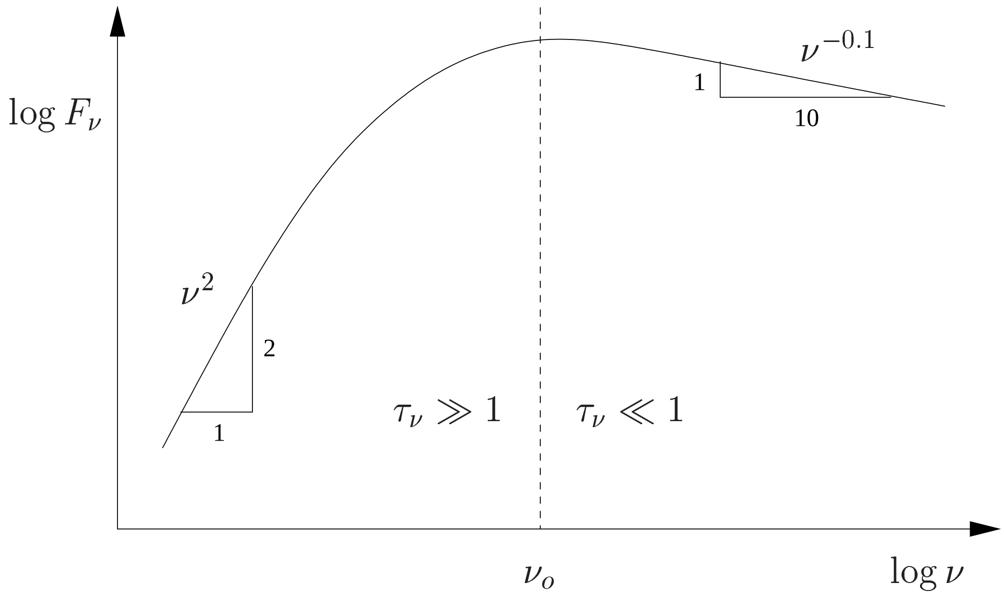

For a typical *compact* HII region, the gas is optically thin above $\nu_o \sim 3\,\mathrm{GHz}$.

Estimates of Physical Parameters

1. Temperature:

   In the optically thick regime, $T_b = T_e$. However, in practice, this is a rather difficult measurement because there could be multiple sources of radiation along the line of sight. For this reason, other methods are preferred, namely, optical spectral lines (forbidden) and radio recombination lines. Note that the measurement of T does not require a knowledge of the distance if we can measure the angle subtended by the source (possible for extended sources like HII regions but not for stars).

2. Electron Density:

   Assume $Z = 1$ (hydrogen). At high ν, we have $\tau_\nu \ll 1$ and the observed flux provides a measure of
   $$\int_V n_i n_e \, dV = \langle n_i n_e \rangle \, V = \langle n_e^2 \rangle \, V$$
   because $n_i = n_e$ if hydrogen dominates (as it usually does). Then, the root-mean-square density is
   $$\langle n_e^2 \rangle^{1/2} = \left(\frac{\int n_i n_e \, dV}{V} \right)^{1/2} \propto \frac{F_\nu^{1/2} D}{V^{1/2}} \propto \left(\frac{F_\nu}{D} \right)^{1/2} .$$
   Unfortunately, in this case, we have to know the distance D to get an estimate for the density.

3. Mass of Ionized Hydrogen:

$$M_{\mathrm{H}} = m_{\mathrm{H}} V \langle n_e^2 \rangle^{1/2} \ .$$

In ionization-bounded HII regions, this is the mass within the Strömgren sphere and, consequently, it is only a *lower bound* to the total mass of hydrogen in the region. For compact HII regions, M_{H} is typically 0.01 to 0.1 $\mathrm{M}_\odot$.

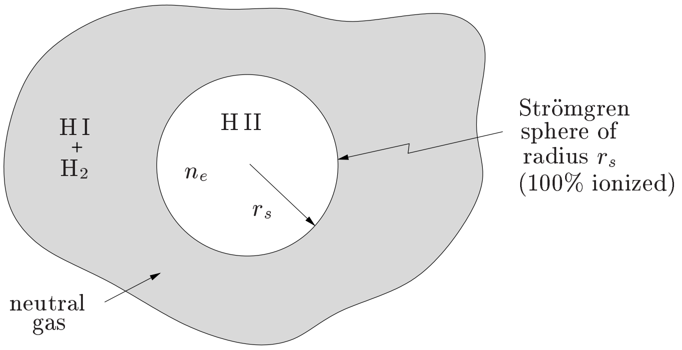

4. Excitation Parameter (see Scheffler & Elsässer p305): The theory of the Strömgren sphere involves the following two quantities:

$$u \equiv r_s \langle n_e^2 \rangle^{1/3} \quad \text{and} \quad L_c \equiv n_e^2 V \alpha_{\mathrm{R}} = \frac{4\pi}{3} u^3 \alpha_{\mathrm{R}} = \quad \text{(ionization equilibrium)}$$

where

$$\begin{aligned} u &= \text{excitation parameter} = \text{constant for a given nebula}, \\ L_c &= \#\ \text{of Lyman continuum photons/unit time (ionization bounded)}, \\ \alpha_{\mathrm{R}} &= \text{recombination coefficient}, \\ r_s &= \text{radius of Strömgren sphere} \propto n_e^{-2/3} \ (\text{for a given } L_c) \ . \end{aligned}$$

Thus, u^3 is a measure of the stellar ionizing luminosity which is responsible for the HII region. Look at this quantity in more detail:

$$u^3 = r_s^3 \langle n_e^2 \rangle = \frac{3}{4\pi} \langle n_e^2 \rangle V = \frac{3}{4\pi} \int_V n_i n_e \, dV \ .$$

Hence, L_c can be related directly to F_ν (radio); that is, in effect, the radio photons are down-converted Lyman continuum photons!

5. Emission Measure:

From $T_b = T_e \tau_\nu$ (optically thin limit), we see that $\tau_\nu = T_b / T_e \propto E_{\mathrm{M}}$ (from p50) and, hence, the emission measure

$$E_{\mathrm{M}} = \int_0^s n_e n_i \, ds' = \langle n_e^2 \rangle \, s$$

can be found *without* knowing the distance. (This assumes that we have already determined T_e in the optically thick frequency limit.) Thus, the scale s of the nebula can be estimated.

Observational Data on HII Regions

The study of bremsstrahlung emission from HII regions has taught us something over the years about the evolutionary development of star-forming regions (which are usually ionization zones due to the presence of young, hot stars). HII regions can be classified according to their electron density. Examine the following table taken from Habing & Israel, *Ann. Rev.*, **17**, 345, 1979. Note the typo at the top of column 4; the unit should be pc cm^{-6}.

Table 3.21 – Classification of H II Regions

Definition				Properties						
Class (1)	n_e(cm^{-3}) (2)	d(pc) (3)	E.M. (pc cm^6) (4)	Nature (5)	Examples (6)	Optical appearance (7)	Group properties (8)	OH/H$_2$O masers (9)	S(20μm)/ S(6cm) (10)	Ionized mass ($M_\odot$) (11)
I	> 3000	< 0.15	> 10^6	Ultra-compact	W3OH, S157B	Obscured	Never isolated	+	< 10^4	$\simeq 10^{-2}$
II	> 1000	0.1–1.0	> 10^5	Compact	W3A, K3-50	Strongly reddened	Never isolated	–	< 10^3	$\simeq 1$
III	100–3000	0.15–10	1×10^4– 3×10^6	Dense	S158, S90	Partially obscured	Sometimes isolated	–	< 5×10^2	$\simeq 10$
IV	100–100	1–30	5×10^2– 1×10^5	Classical	S104, S162	Globules, bright rims	Sometimes in groups	–	< 10^2	$\simeq 10$–5×10^2
V	3–50	10–300	< 5×10^5	Giant	Core, NGC5461	Complex or diffuse	—	–	–	$\simeq 500$–5×10^6
VI	10	> 100	< 1×10^5	Super-giant	Envelope, NGC5461	Structure-less	—	–	–	$\simeq 10^6$–10^8

[a] From Israel (1976b).

The theory of Strömgren spheres tells us that

$$n_e^2 r_s^3 = u^3 = \text{constant (fixed } L_c) \ .$$

Therefore,

$$(n_e^2 r_s) r_s^2 = \text{constant}$$

or

$$E_{\rm M} = n_e^2 r_s \propto r_s^{-2} \ .$$

Also,

$$n_e \propto r_s^{-3/2}$$

or

$$M \propto n_e r_s^3 \propto r_s^{3/2} \propto n_e^{-1} \ .$$

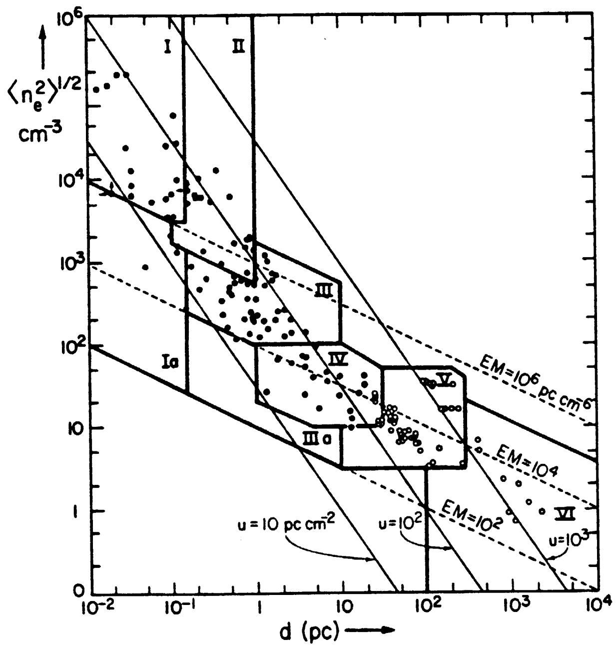

Figure 3.2 – Plot of rms electron density (n_e) versus linear size (d or r_s) for individual H II region components. Lines of constant excitation parameter (u) and constant emission measure (EM) are marked. Filled circles are galactic H II region components, open circles are extragalactic components, all observed with the Westerbork Synthesis Radio Telescope. Heavy lines and Roman numerals indicate the classification scheme outlined in Table 3.21. (From Israel 1976b.)

Table 3.22 – Examples of compact H II regions which are contained in larger objects. The quoted positions and angular sizes of the individual sources were obtained by interferometric observations in the cm wave region. (From Scheffler & Elsässer.)

Extended object	Compact components	α_{1950}	δ_{1950}	Angular diameter [arc s]	Distance [kpc]	Linear diameter [pc]
W3 (with opt. nebula IC 1795)	A1–A5	$2^h21^m56^s.6$	$+61°52'43''$	28 ... 35		0.4 ... 0.5
	C	$2^h21^m43^s.6$	$+61°52'46''$	5	3.1	0.071
	W3(OH), comp. *A*	$2^h23^m16^s.5$	$+61°38'57''$	1.5		0.024
M42	Ori *A*, G 209.0–19.4	$5^h32^m50^s$	$-5°25'15''$	240	0.5	0.6
M8	A1 (Ring)	$18^h00^m37^s.0$	$-24°22'50''$	15	1.4	0.10
	A4	$18^h00^m36^s.3$	$-24°22'52''$	46		0.32
M17	S	$18^h17^m34^s$	$-16°13'24''$	220		2.3
	N	$18^h17^m39^s$	$-16°10'30''$	280	2.1	2.9
	E	$18^h17^m51^s$	$-16°11'30''$	190		2.0
W51	G 49.5–0.4*d*	$19^h21^m22^s.3$	$+14°25'15''$	11	7.3	0.4
	e	$19^h21^m24^s.4$	$+14°24'43''$	19		0.7
W75	DR 21 *A*	$20^h37^m13^s.7$	$+42°08'55''$	5.7		0.083
	B	$20^h37^m14^s.0$	$+42°09'03''$	4.0	3.0	0.058
	C	$20^h37^m14^s.1$	$+42°08'54''$	7.1		0.101
	D	$20^h37^m14^s.2$	$+42°09'15''$	4.2		0.062
NGC 7538 = S 158	A1	$23^h11^m30^s.3$	$+61°12'56''$	110		1.4
	A2	$23^h11^m20^s.8$	$+61°13'45''$	10	2.5	0.12
	B	$23^h11^m36^s.7$	$+61°12'00''$	12		0.15
	C	$23^h11^m36^s.7$	$+61°11'50''$	1.0		0.013

Table 3.23 – Mean electron temperature T_e, emission measure E, root mean square electron density $\overline{N_e^2}^{1/2}$, excitation parameter u, total number of Lyman continuum photons per second L_c, and total mass of ionized hydrogen M(HII) for a selection of H II regions.

Object	T_e [K]	E [pc cm^{-6}]	$(\overline{N_e^2})^{1/2}$ [cm^{-3}]	u [pc cm^{-2}]	L_c [s^{-1}]	$\mathcal{M}$(H II) [$\mathcal{M}_\odot$]
W 3, A1-A5	8400	2×10^7	6×10^3	83	4×10^{49}	10
W 3(OH)	10000	1×10^9	2×10^5	54	3×10^{48}	0.1
M 42	8200	6×10^6	5×10^3	55	7×10^{48}	10
NGC 2237-46	8000	3×10^4	20	80	2×10^{49}	1×10^4
M 20	8000	5×10^4	1×10^2	50	5×10^{48}	2×10^2
M 8	8000	4×10^5	6×10^2	64	1×10^{49}	2×10^2
M 17, main source (S)	7700	5×10^6	2×10^3	170	2×10^{50}	10^2
M 16	8000	4×10^5	2×10^2	120	7×10^{49}	7×10^2
W 51, main source	7300	5×10^7	8×10^2	190	3×10^{50}	10^2
W 75, DR 21 A		5×10^7	2×10^4	36	2×10^{48}	0.2
B	8400	5×10^7	3×10^4	27	7×10^{47}	0.1
C		9×10^7	3×10^4	49	4×10^{48}	0.4
D		4×10^7	3×10^4	27	7×10^{47}	0.1
NGC 7538 A1		8×10^5	1×10^3	60	8×10^{48}	33
A2	7900	2×10^6	4×10^3	14	1×10^{47}	0.1
B		7×10^6	6×10^3	26	7×10^{47}	0.3
C		1×10^7	1×10^5	12	7×10^{46}	0.002
NGC 7000	7000	4×10^3	10	100	4×10^{49}	2×10^4

Table 3.24

Broad classification scheme for the H II regions (after a suggestion by Churchwell 1975).

Name of the object observed	Observed characteristics	Diameter [pc]	N_e [cm^{-3}]	Stage of development	Examples
Compact infrared source at $\approx 20\,\mu m$	Continuous emission at $\simeq 20\,\mu m$, but not at $2\,\mu m$; no radio continuum; optically not detectable	$\lesssim 0.05$	$>5 \times 10^3$	Pre-Main Sequence O-star in a shell, opaque to optical radiation, including UV ("cocoon star")	IRS 5 in W 3
Compact H II region	Thermal radiocontinuum; infrared continuum; usually not detectable in the visible	0.05...1	$\gtrsim 10^3$	Earliest phase of development of an H II region	Components in W 75, DR 21 and in NGC 7538 (see Table 4.10)
Complex H II region of intermediate density	Continuous and line radiation in the optical, infrared and radiofrequency regions	1...100	$10 \ldots 10^3$	Expanding H II region	M 42, M 17
Large diffuse H II region		>100	$\lesssim 10$	Very far expanded H II region	NGC 7000 (North America Nebula)